Near Field Measurements of an Axisymmetric Turbulent Jet at Low Reynolds Numbers: A PIV and CTA Comparison

[1]Brian D. Landers, [2]Peter J. Disimile

[1,2]Department of Aerospace Engineering, University of Cincinnati, Cincinnati, OH, USA 45221

Abstract—This paper presents a comparison between two commonly used velocity measurement techniques applied in experimental fluid dynamics: Constant Temperature Anemometry (CTA) and Particle Image Velocimetry (PIV). Previous studies have applied these techniques to the self-similar region of an axisymmetric jet which resides in the far-field. However, there is a lack of CTA to PIV comparison data in the near-field region of the jet where the flow field contains large scale turbulent structures. The following comparison is performed in the near-field region of an axisymmetric circular turbulent jet at five Reynolds numbers based on diameter between 5,000 to 25,000. The Reynolds numbers were selected in order to cover the critical Reynolds number range, 10,000 to 20,000, where the characteristics of the flow transition to a fully developed turbulent mixing layer. A comparison between these two measurement techniques was performed in order to determine the differences between an intrusive (CTA) and non-intrusive (PIV) method when applied to a practical application. The axial mean velocity and u_{rms} level show qualitative agreement between these two measurement techniques for all 5 Reynolds numbers; however, there is a quantitative discrepancy of up to 18% in the mean velocity and over 40% in the turbulent velocity.

Index Terms—Particle Image Velocimetry, Constant Temperature Anemometry, Hotwire Anemometry, Axisymmetric Turbulent Jet, Near-Field Measurements

I. INTRODUCTION

Turbulent jets are of great importance in fluid dynamics and heat transfer and are typically found in aerodynamics, chemical mixing, and thermal management applications. Considerable research has been performed experimentally as well as theoretically in order to understand different aspects of the mixing process throughout the flow field involving turbulent jets. The most common jet used for research has been the axisymmetric jet. The axisymmetric jet is comprised of three regions based on the velocity field: the near-field, the transition, and the far-field regions. The near-field is the region where the characteristics of the flow downstream of the exit (z-direction) are similar to the characteristics of the flow at the jet exit. This near-field region usually spans from $0 \leq z/D \leq 6$. The far-field region is the region in which the flow becomes self-similar and has reached a dynamic equilibrium. A self-similar flow is a flow whose shape does not change with distance. In the far-field region, the velocity and turbulence profiles change character become self-similar and fully developed. This region usually spans beyond $z/D \geq 25$. The transition region, $6 \leq z/D \leq 25$, comprises of the region between the near- and far-fields of the flow. The far-field region of the jet is greatly influenced by the nascent portion of the jet located in the near- and intermediate-fields.

The mixing of the near-field region is shown to change significantly in the range of critical Reynolds numbers which spans from 10,000 to 20,000. The characteristics of the jet flow transition from the early stages of an axisymmetric jet with a well-defined core and a surrounding annular shear layer to a more well-mixed state of homogenous turbulence. Dimotakis et al [1] quantitatively characterized the mixing transition of the near-field region for a circular jet through the use of flow visualization and quantitative observations.

The majority of previous measurements have focused on the self-similar region which resides in the far-field. Studies performed for the purpose of comparison of PIV to Hot-wire anemometry have only been undertaken for the transitional and far-field regions. Diodati et al.[2] made a comparison of laser-doppler velocimetry, hot-wire anemometry, and particle image velocimetry (PIV) for the investigation of a turbulent jet with a Reynolds number of 68,000 at a range of axial positions ($10.6 \leq z/D \leq 12$) downstream of the jet exit. Burattini et al. [3] investigated the corrections needed to be applied to PIV and CTA data in the far-field of two round jets. These PIV and CTA measurements were made for a Reynolds number of 20,000 based on pipe diameter, at a range of axial positions, z/D, from 25 to 30.

Constant temperature anemometry (CTA) measurements have been performed in the near-field as well as the transition region for a wide variety of Reynolds numbers. The general procedure and results from these investigations are summarized in the following paragraphs.

The effect of Reynolds number on the near- and transition regions ($0 \leq z/D \leq 25$) of a round free jet was investigated by Fellouah et al.[4] Flying and stationary hotwire measurements were carried out for exit Reynolds numbers of 6,000, 10,000, and 30,000. The objective was to determine the differences in velocity profiles and turbulence intensity profiles at the various Reynolds numbers. The results showed that at all Reynolds numbers the inertial span of the turbulent intensity increases with distance downstream from the jet exit.

Jung et al. [5] performed an experiment in an axisymmetric turbulent jet. Data was collected using the hotwire probe designed by Citriniti and George and consisted of 138 individual hotwires placed in six concentric circles. Hot-wire measurements were carried out for exit Reynolds numbers of 78,400, 117,600, and 156,800 at a range of axial positions, z/D, from 2 to 6. The proper orthogonal decomposition (POD) was applied, using an in-house software program, to perform a double Fourier transform and determine the resulting modes. Full-field streamwise velocity analysis of the POD modes showed the evolution of flow with downstream position, in the form of a 'volcano-type' to a 'propeller-like' pattern.

Ferdman et al. [6] measured the effects of non-uniform initial velocity profiles on the downstream evolution of round turbulent incompressible jets. These hotwire measurements were used to determine the velocity of two jets, one with an axisymmetric fully developed profile and the other with an asymmetric initial profile where the jet is non-uniform due to the shape of the jet. Both jets had a Reynolds number of 24,000 based on the exit bulk velocity and source diameter. Measurements were taken down stream at axial positions, z/D, from 0 to 80. These results showed that the growth of initial turbulent intensity is greater for the jet with the uniform initial velocity profile.

Particle Image Velocimetry (PIV) measurements have also been made in near-field and transition regions for a wide variety of applications at various Reynolds numbers. Results vary due to the importance of seeding the flow, as discussed in the next section of this paper. The results and procedures from these PIV studies are summarized in the following paragraphs.

Milanovic et al. [7] preformed PIV to obtain reliable statistics in the near-field region of a submerged turbulent water jet. PIV was used to measure the mean axial velocity and RMS velocity for Reynolds numbers at the exit of the pipe of 14,602, 19,135, and 24,685 at a range of axial positions, between z/D of 1 to 8. The Reynolds numbers were selected to overlap the critical Reynolds number range of 10,000 to 20,000. The results show that the mean axial and radial velocities are independent of Reynolds number but the axial RMS component was found to increase as the Reynolds number was increased.

PIV measurements were also performed at the exit and initial region of the near-field ($0 \leq z/D \leq 2.2$) of a water jet by Shinneeb et al.[8] Similar to Jung et al.[5], Shinneeb et al. used proper orthogonal decomposition (POD) analysis on the fluctuating velocity fields to investigate the large-scale structures of the flow with an exit Reynolds number of 22,500. These results show the creation of alternating direction vortices which begin to be resolved at a streamwise location of one half the diameter of the jet. Also shown, the vortices grow linearly in number in the downstream direction up to one jet diameter downstream.

Ganapathisubramani et al. [9] used stereo PIV techniques to measure all three velocity components in the developing shear layer. PIV measurements were made in the near-field region ($0 \leq z/D \leq 1.8$) of a round jet at a Reynolds number of 19,000. The results show axial and radial RMS velocity values are high in the shear layer and low in the potential core of the jet. Also, the azimuthal RMS velocity increased as the distance downstream from the exit increased and reached a maximum in the shear layer.

As shown above, there is a lack of measurement data comparison between Constant Temperature Anemometry (CTA) and Particle Image Velocimetry (PIV) in the near field of an axisymmetric jet in a range of Reynolds numbers spanning the critical Reynolds numbers previous described. Previous data has shown that CTA and PIV techniques have not always been in agreement with one another. The objective of the current work is to analyze and compare the measurement results of CTA and PIV in the near-field of an axisymmetric turbulent jet. The axial mean and RMS velocities were acquired with both CTA and PIV measurement techniques for five Reynolds numbers: 5,000, 10,000, 15,000, 20,000, and 25,000. The current measurements will span radially from -1.5D to 1.5 at three downstream axial locations, z/D: 2, 4, and 6.

II. MEASUREMENT METHOD OVERVIEW

A. Constant Thermal Anemometry

Constant temperature anemometry (CTA), also known as thermal anemometry, is an intrusive measurement technique used to measure the velocity and turbulence in 1, 2, or 3-dimensional gas or liquid flows, using hot-wire or hot-film probes inserted into the flow. The advantage of a hotwire comes from their small size, which enables very good spatial resolution and high frequency response to over 100 kHz. The calibration of a hotwire is crucial to the accuracy of the velocity and turbulence measurements. The calibration standard typically uses a Pitot tube connected to a pressure transducer. The hotwire is placed in the center of a reference flow, and carefully oriented along the flow direction. The Pitot tube measures the difference in static and dynamic pressures in the flow. The velocity is then calculated from the measured pressure difference as shown below:

$$\Delta P = \frac{\rho U^2}{2} \qquad (1)$$

Correlating the output signal to velocity using the Collis and William's relation and a least-squared regression, the constants A, B, and n are determined as shown in the following equation. By applying these constants, the hotwire can now be used to make accurate velocity measurement at a point within the range of calibration.

$$E^2 = A + BU^n \quad (2)$$

The CTA system sensing element consists of a small heated wire which is electrically heated to a pre-specified temperature greater than the surrounding air. The associated instrumentation electronics transforms changes in the sensor resistance, resulting from the surrounding fluid flowing over and cooling the wire, into a useful signal. A typical hotwire is 5 microns in diameter and approximately 1 mm in length. Further information on CTA systems and hot-wire probes can be found in Jorgensen [13]. The CTA measurement system determines the fluid velocity by the amount of heat being lost from the wire, which is held constant at an elevated temperature to the cool surrounding fluid. The heat transferred is a direct function of the flow velocity. In theory, as the velocity increases the convective heat transfer coefficient will increase causing the wire temperature to begin to decrease; however, the instrumentation electronics senses this change and supplies more current to the wire to counteract this change and thereby maintain the wire at a constant temperature. The CTA systems provide time accurate velocity data at a single spatial location which can be post processed to determine the mean velocity and turbulence intensity at that point.

B. Particle Image Velocimetry

The Particle Image Velocimetry (PIV) measurement technique is a non-intrusive, optical method based on flow visualization that is used to obtain 2-dimensional full-field measurements. PIV involves seeding the flow with micron sized tracer particles whose speed will be determined and assumed to accurately follow the flow dynamics. The tracer particles are then illuminated, usually with a high energy pulsed laser light sheet, so only the tracer particles in the 2-dimensional field are made visible. A high speed imaging device, synchronized with the pulsed light sheet than captures a single image per laser pulse. The camera and laser are set to a pre-specified image acquisition rate allowing the capture of multiple images with a few hundred nanoseconds (ns) between them. The velocity of the tracer particles is then determined using time between images and the corresponding particle displacement as shown in the equation below:

$$V = \frac{\Delta X}{\Delta t} \quad (3)$$

A spatial calibration on the pixel scale of the imaging device is needed to produce accurate velocity measurements and particle sizes. The velocity calculations are typically determined by pixel displacement through the use of particle tracking software algorithms. Various types of algorithms and filters may be applied to the images in order to obtain optimal particle tracking.

Seeding of tracer particles in the flow is the most critical component of the PIV measurement system. Ideally, the tracer particles will be spherical in shape and have approximately the same density as the fluid; hence the particles will be neutrally buoyant in the flow. The particle size is typically between 10 to 100 microns depending on the flow under study. These particles need to be small enough to accurately follow the flow dynamics, but large enough to scatter sufficient levels of incident laser light to be seen by the camera. In order to determine how well the tracer particles follow the flow dynamics, the effective Reynolds number can be calculated as follows:

$$Re_e = \frac{\rho_g |V_g - V_p| D}{\mu_g} \quad (4)$$

The effective Reynolds number essentially shows the difference in Reynolds numbers between the fluid and the tracer particles. Seeding is most commonly introduced to the flow by the generation of solid particles from powders. This can be achieved by either a global technique where the particles are introduced into the flow well upstream of the region of measurement, or through a local technique where the particles are introduced to a restricted portion of the flow field that is to be measured.

Once the images are captured they must be analyzed in order to determine the instantaneous 2-dimensional velocity. Each image is split into a large number of interrogation windows. Interrogation windows are small cross-sectional areas superimposed on the image that enable the analysis of individual particles to produce a single particle for each window. Cross-correlation techniques are then used to compute a displacement vector for each interrogation window. To more accurately measure the flow, an overlap of interrogation windows can be applied. On average, the interrogation window should be selected to have between 5 and 15 particles per window. The image capture frame rate of the camera can be controlled to allow for a certain amount of time between successive images. For accurate PIV measurement analysis, the frame rate should be set so the average particle displacement between successive images is between 5 and 15 pixels.

III. EXPERIMENTAL STRATEGY

A. Test Setup

The system used in the current study is comprised of an air compressor, an air supply reservoir, a flow regulator, a settling tank, a fluidized bed, and a jet. The air supply reservoir consists of two tanks connected in series, having volumes of 200 and 50 gallons respectfully. A compressor is used to charge the tank reservoir to a pressure of 140 psi in order to deliver the necessary flow rates needed for the desired Reynolds numbers. A settling tank is connected downstream of the regulator to allow for the flow to dampen out and eliminate any pulsations in the flow. A spherical fluidized bed is connected after the settling tank to enable the introduction of seeding particles before the flow enters the jet as shown in Figure 1. The jet was produced using a black iron pipe with an inner diameter D=19.05 mm (0.75 in), a length of L=914.4 mm (36 in.), and a wall thickness of 3.175 mm (0.125 in.). The pipe was sufficiently long to enable the flow to become fully developed and turbulent at the exit of the pipe based on the length-to-diameter ratio of the pipe, L/D=48.

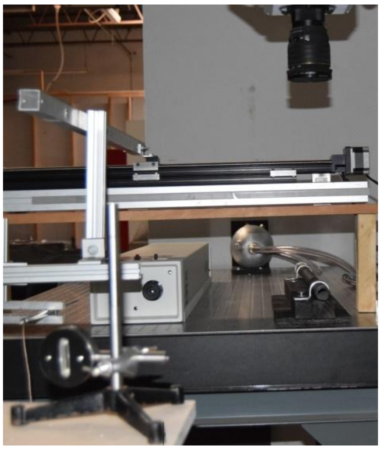

Figure 1: CTA and PIV Test Setup

Figure 2 shows that the origin of the cylindrical coordinate system, r, z, used in this study is located on the centerline at the exit plane of the pipe. For the current study the jet was assumed to be axisymmetric and hence no circumferential components were expected, therefore only r and z dimensions are needed.

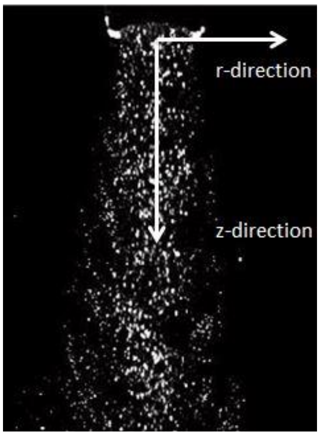

Figure 2: Coordinate System

CTA and PIV measurements were made for the following five Reynolds numbers: 5,000, 10,000, 15,000, 20,000, and 25,000. The flow rate through the jet was controlled by a pressure regulator which held constant the following average velocities corresponding to each Reynold number as follows: 4.1 m/s, 8.3 m/s, 12.4 m/s, 16.6 m/s, and 20.7 m/s. Measurements were made at the following downstream axial locations, z/D, from the jet exit: 0, 2, 4, and 6. Measurements were taken in the radial direction ($-1.5 \leq r/D \leq 1.5$) at each of these axial locations.

B. CTA System Configuration and Operation

A Dantec Dynamics constant temperature anemometry system was used to measure the axial velocity of the flow along each r-z plane of interest. The system consisted of a Dantec hot-wire probe, probe holder, and a Dantec CTA standard bridge type 55M10. The output voltage from the CTA was then processed using LabView, a data acquisition program.

In the present study, the CTA system was used to measure the flow along the r-direction in the r-z plane at the following z/d positions: 0, 2, 4, and 6. At each of these downstream locations, 100 evenly spaced data points were taken in the r-direction. An electronically controlled traverse was used in order to accurately move the probe to each desired location. The measurements were centered on the coordinate system at the pipe exit and span from $-1.5 \leq r/D \leq 1.5$. The data was acquired at each location at sampling rates of 10 kHz for a period of two seconds resulting in an averaged velocity of 20,000 data points. Also, a settling time of 3 seconds was incorporated between each traverse movement in order for the probe to become stationary before acquiring new data.

C. PIV System Configuration and Operation

A two-dimensional PIV system was used in the current study to measure the flow field along the r-z plane extending from the pipe exit. The system consisted of a light source, high speed imaging device, fluidized bed, seeding particles, and a data analysis program. The light source was a Lexel 95-3 Argon Ion laser system. The laser was capable of operating up to 3 Watts of power. A Photron SA1.1, 1 megapixel high-speed camera capable of taking more than 5,000 frames per second (fps) at full resolution (1024 x 1024 pixels) was used in the current study. The frame rate used changed depending on the Reynolds number, which was between 5,000 and 20,000. It was critical to set the correct frame rate and shutter speed in order to ensure clear, crisp images.

The Lexel 95 Argon Ion laser operating in single line mode (514.5 nm wavelength) produces a green beam 1.5 mm in diameter. The beam is reflected off a mirror and passes through light sheet forming optics, consisting of spherical and cylindrical lenses, in order to generate a thin, focusable light sheet as shown in Figure 3. The light was generated horizontally at the pipe exit to illuminate the r-z plane of interest. The thickness of the light sheet at the jet exit was 500 microns. The location of the lighting system remained fixed throughout the entire study. The Photron camera was placed perpendicular to the light sheet. The lens used was a 20mm F1.8 DG Macro by Sigma. An f-stop of 4.0 was used for the PIV images in the current study.

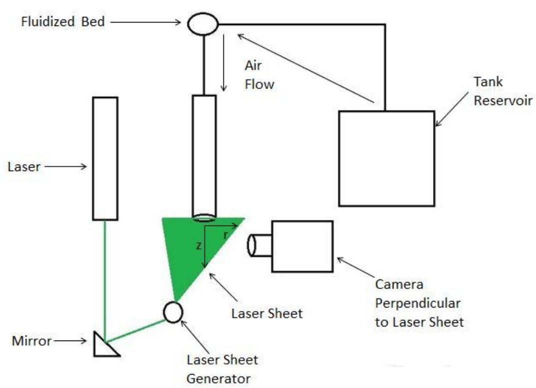

Figure 3: PIV Test Setup

The seeding particles selected had 10-15 micron diameters. Dry powder was selected due to the density of each particle being near that of the fluid of interest, resulting in the particles being nearly neutrally buoyant in the flow.

OpenPIV, an open source program written in MATLAB, was used as the data analysis program to compute the velocity vectors determined from the displacement of particles in consecutive images. More information about OpenPIV can be found in the paper by Taylor et al.[14]

Each image was separated into multiple interrogation windows where a cross-correlation technique was applied to evaluate the velocity vectors by calculating the particle displacement between consecutive images. The interrogation window selected for the current study extended 32 x 32 pixels with a 50% overlap area of 16 x 16 pixels.

In order to account for outliers, a filter was applied to eliminate any velocity vectors that were greater than 25 times the local standard deviation. After each iteration, a local comparison of vector characteristics is performed in order to validate and remove outliers. At each Reynolds number, 3,000 images were averaged to evaluate the mean and RMS flow fields. The CTA was used to set the correct centerline axial velocities needed for the Reynolds numbers of the current study.

IV. RESULTS

Figure 4a and 4b show the radial profiles of the mean axial velocities at the exit of the pipe, measured using PIV and CTA respectfully, compared to the hotwire data obtained by Xu and Antonia [15] for all five Reynolds numbers: 5,000, 10,000, 15,000, 20,000, and 25,000. All the velocities were normalized by the centerline axial velocity, U_c, and the radial distances are normalized by the pipe diameter, D.

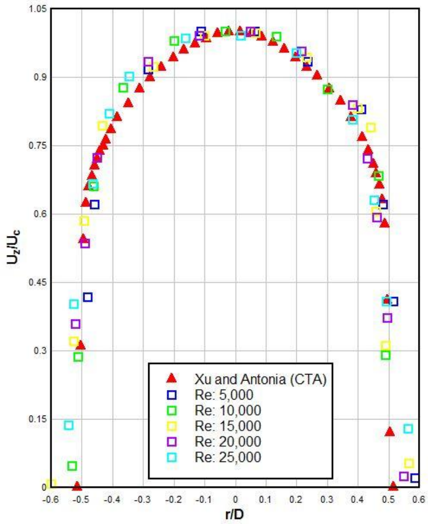

Figure 4a: PIV radial profiles of the axial velocity (U_z/U_c) at the pipe exit compared to previous literature data at all five Reynolds numbers

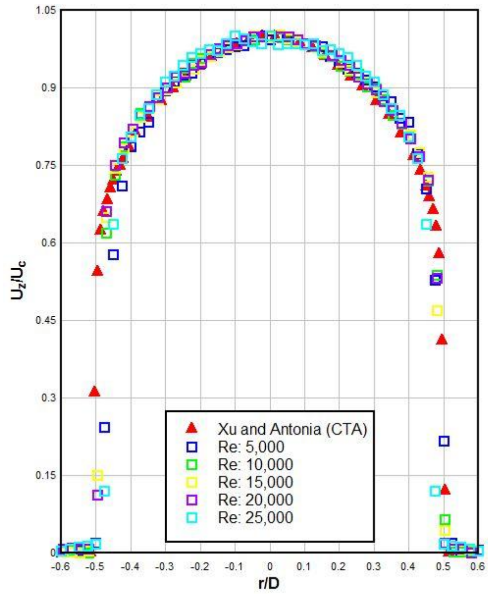

Figure 4b: CTA radial profiles of the axial velocity (U_z/U_c) at the pipe exit compared to previous literature data at all five Reynolds numbers

Figure 5 show the mean axial velocity, U_z, contours of the jet at Reynolds numbers of 15,000 between z/D = 0 and 10. The mean axial velocity has been normalized by the mean centerline velocity, U_z/U_c. The velocity contour in Figure 5 is an average of the PIV analysis of 3,000 consecutive images.

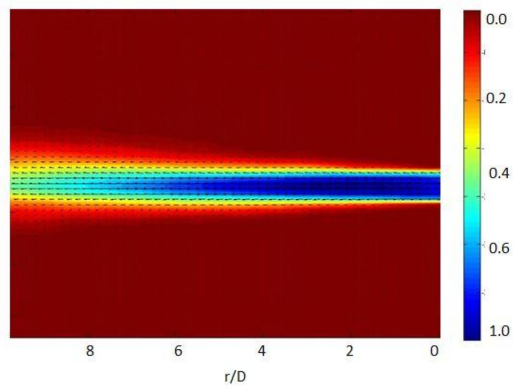

Figure 5: Mean axial velocity contour normalized by the centerline velocity (U_z/U_c) between z/D = 0 and 10

Figures 6 and 7 illustrate the radial profiles of axial mean velocity at four downstream locations of Reynolds numbers: 10,000 and 20,000 respectfully. The velocity is normalized by the centerline velocity, U_c, at each axial location. The maximum axial mean velocity discrepancy between the PIV and CTA measurements is lowest for a Reynolds number of 10,000 and highest for a Reynolds number of 20,000 as shown in Figure 6 and 7, out of the five Reynolds numbers measured in the current study.

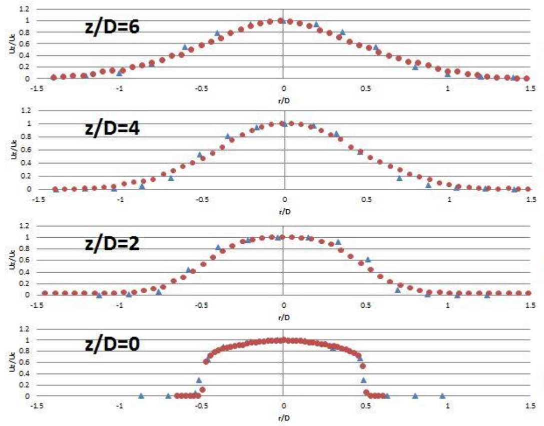

Figure 6: Radial profiles of the mean axial velocity (U_z/U_c) at four axial locations downstream for Reynolds number: 10,000

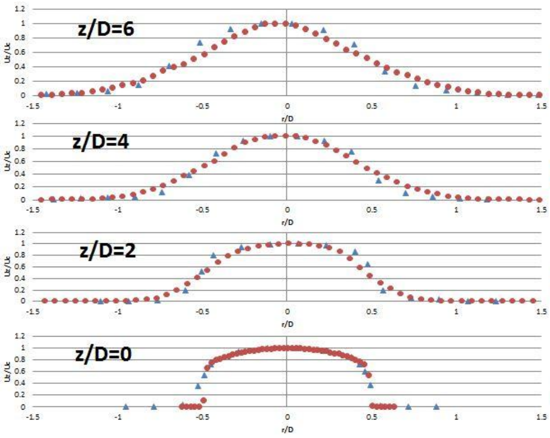

Figure 7: Radial profiles of the mean axial velocity (U_z/U_c) at four axial locations downstream for Reynolds number: 20,000

Figures 8 and 9 illustrate the radial profiles of u_{rms} velocity at four downstream locations with Reynolds numbers: 25,000 and 10,000 respectfully. The maximum u_{rms} velocity discrepancy between the PIV and CTA measurements is highest for a Reynolds number of 25,000 and lowest for a Reynolds number of 10,000, as shown in Figures 8 and 9, out of the five Reynolds numbers measured in the current study.

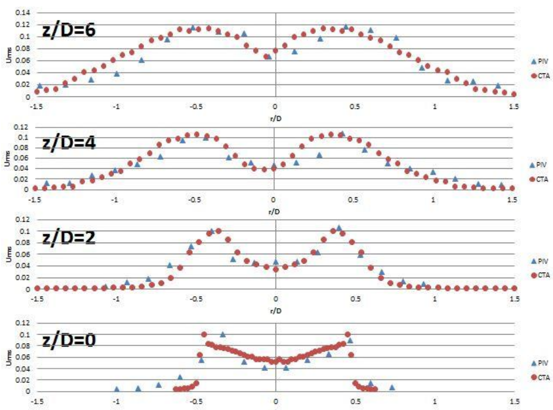

Figure 8: Radial profiles of the U_{rms} velocity at four axial locations downstream for Reynolds number: 25,000

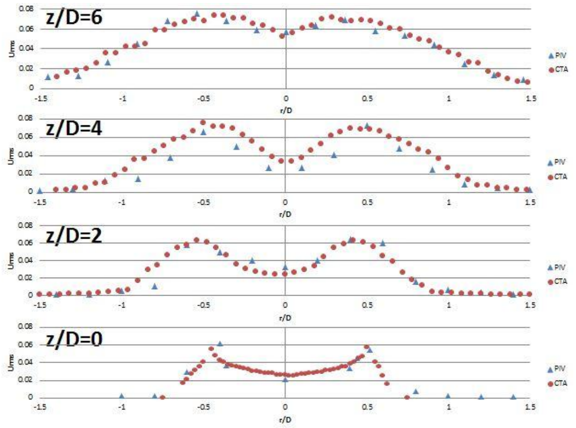

Figure 9: Radial profiles of the U_{rms} velocity at four axial locations downstream for Reynolds number: 10,000

V. DISCUSSION

The axial mean and u_{rms} velocities are presented to provide insight into how well non-intrusive PIV measurement systems agree with intrusive CTA measurement systems for an axisymmetric turbulent jet in the near field at Reynolds numbers between 5,000 and 25,000.

Figure 4a and 4b show that the measurements of the PIV and CTA systems obtained in the current study follow a similar trend at the jet exit to the CTA measurements by Xu and Antonia.[15] However, the CTA measurements are in slightly better agreement with the CTA measurements of Xu and Antonia when compared to the PIV measurements.

As can be seen in Figure 5, the potential core length of the jet measured by the PIV system exists from the exit of the jet up to z/D=4.4. The potential core is typically the region of flow where $U/U_c \geq 0.9$. CTA measurements indicate the potential core of the jet existing up to z/D=4.6. The PIV data suggest a potential core approximately 4.5% longer than that determined by the CTA measurements.

The general qualitative trend of the axial mean and u_{rms} velocity profiles for both the PIV and CTA systems are similar; however, there is a quantitative discrepancy between the axial values at corresponding radial locations. This discrepancy occurs at the exit of the jet and is influenced by the shear layer and will be discussed in detail in the next paragraph. For the mean velocity measurements, Figure 6 illustrates the Reynolds number (10,000) where the maximum difference between the two systems is the lowest and approaches 10%. On the contrary, Figure 7 shows the Reynolds number (20,000) where the maximum difference in the mean velocity measurement between the two systems is the highest at up to 18%. For the u_{rms} velocity, Figure 8 illustrates the Reynolds number (25,000) where the maximum difference between the two systems is the lowest at up to 22%. Also, Figure 9 shows the Reynolds number (10,000) where the maximum difference in the u_{rms} velocity measurement approaches 41%. There is no direct correlation between the Reynolds number or the axial distance downstream and the agreement between the two systems.

As can be seen in Figures 6 through 9, the greatest discrepancy between the two measurement techniques occurs in the shear layer. This discrepancy can be seen at all of the downstream axial locations but is most prevalent at the pipe exit. The discrepancy also is shown to be much greater in the shear layer of the u_{rms} velocity than the mean velocity. This is thought to be caused by the difference in spatial resolution between the two measurement techniques.

In the current study, the CTA measurements were sampled at a rate of 10 kHz for two seconds at each radial location with a 1 mm interval between radial locations. Also, the hotwire diameter was 5 microns. At the exit, the CTA system was able to provide much greater spatial resolution, that is provide data at 75 radial locations across the area of interest with each average data point being represented by an average of 20,000 samples.

The PIV measurement system used a cross correlation technique, as shown in Figure 10, to calculate the instantaneous velocity of each particle in each interrogation window. These values were then used to calculate an average displacement vector for each window.

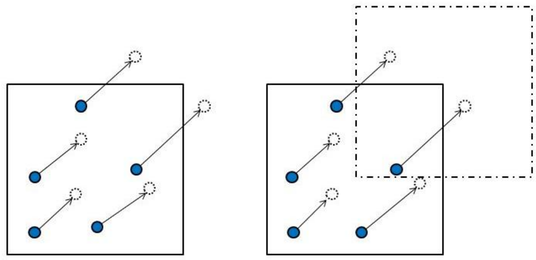

Figure 10: PIV cross correlation (left) and adaptive correlation (right) measurement methods

Due to this technique, the spatial resolution must be maximized in order to get the most accurate results using a PIV measurement system. In order to obtain the maximum amount of points through the area of interest, the area of interest must occupy a large portion of the image as shown in Figure 11. If the interrogation window and image pixel size remains the same for both drawings (Figure 11) it can be seen that when the area of interest is doubled in the radial direction the amount of data points through the area of interest is also doubled from 5 to 10.

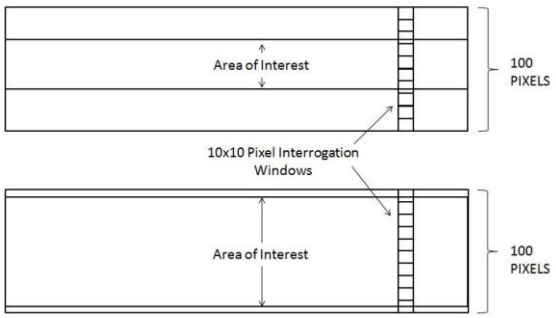

Figure 11: Spatial resolution based on area of interest

One of the main causes for the discrepancy between the two techniques in the shear layer is due to interrogation window size. If the interrogation window size is too large, the average displacement vector will not provide an accurate representation of the instantaneous velocity at that location. As shown in Figure 12, at some locations throughout the shear layer, especially near the pipe exit where the shear layer is thin, the velocity is being averaged with values both inside the shear layer, and within the potential core since these regions resided within a single interrogation window and therefore results in a misrepresentation of the velocity at that location. However, this can be corrected by decreasing the interrogation window and by also increasing the spatial resolution, making sure the area of interest occupies the majority of the image as shown in Figure 11. By doing this, it will allow for the shear layer to require a greater number of pixels and thus allow for more interrogation windows inside the shear layer. This is most critical when the shear layer is small. However, one must be careful when reducing the interrogation window size if trying to accurately calculate the u_{rms} velocity. It was discovered that if the interrogation window is too small, the u_{rms} velocity will be much higher because each interrogation window will have less particles to calculate an average displacement vector resulting in higher standard deviations.

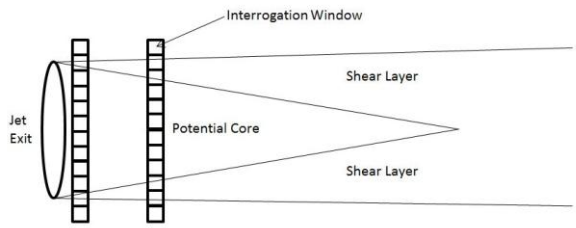

Figure 12: PIV through the shear layer of the flow

For the current study, the quantitative discrepancy between the results is believed to be attributed to the difference between the data acquisition strategy of the two measurement techniques. The CTA system at each radial location takes an average of 20,000 data points; whereas the PIV system takes an average of 3,000. The CTA system had an acquisition area of 5 microns; whereas the PIV system had an acquisition area of 5 mm (32 pixels). This resulted in the CTA system being able to measure 75 data points across the flow at the jet exit while the PIV system was only able to measure 25 resulting in considerable spatial averaging.

VI. CONCLUSION

The axial mean and u_{rms} velocities show a general qualitative agreement between the two measurement techniques for all 5 Reynolds numbers; however, there is a significant quantitative discrepancy. The discrepancy in the axial mean velocity between the two techniques was found to be 18%; whereas the discrepancy in u_{rms} velocity approached 41%. This discrepancy is most severe in the shear layer near the pipe exit and impart due to the difference in spatial resolution between the two measurement techniques. This research suggests that when using a PIV measurement technique, care must be taken to ensure proper seeding, spatial resolution and post processing configuration to ensure accurate results.

ACKNOWLEDGEMENTS

The authors are grateful to Mrs. Veronica Disimile and Engineering and Scientific Innovations Inc. for allowing us to use their facility to perform the current study.

REFERENCES

[1] Dimotakis, P. E., Miake-Lye, R. C., and Papantoniou, D. A., 1983, ‘Structure and Dynamics of Round Turbulent Jets,’ Phy. Fluids, **26**, pp. 3185-3192.

[2] Diodati, P., Paone, N., Rossi, G. L., and Tomasini, E. P., 1993, ‘Comparison of Laser Doppler Velocimetry, Hotwire Anemometry and Particle Image Velocimetry for the Investigation of a Turbulent Jet,’ SPIE, **2052**, pp. 315-322.

[3] Burattini, P., Falchi, M., Romano, G. P., and Antonia, R. A., 2010, ‘PIV and Hot Wire Measurements in the Far Field of Turbulent Round Jets,’ Meas. Sci. Technol.,**21**, pp. 125402-125417.

[4] Fellouah, H., Ball, C. G., and Pollard, A., 2009, ‘Reynolds Number Effects Within the Development Region of a Turbulent Round Free Jet,’ Int. J. Heat and Mass Transfer, **52**, pp. 3943-3954.

[5] Jung, D., Gamard, S., and George, W. K., 2004, ‘Downstream Evolution of the Most Energetic Modes in a Turbulent Axisymmetric Jet at High Reynolds Number. Part 1. The Near-Field Region.’ J. Fluid Mech., **514**, pp. 172-204.

[6] Ferdman, E., Otugen, M. V., and Kim, S., 2000, ‘Effect of Initial Velocity profile on the Development of the Round Jets,’ J. Propulsion and Power, **16**, 4, pp. 676-686.

[7] Milanovic, I. M., and Hammad, K. J., 2010, ‘PIV Study of the Near-Field Region of a Turbulent Round Jet,’, Canada, August 1-5, Paper 31139.

[8] Shinneeb, A. M., Bugg, J. D., and Balachandar, R., 2008, ‘Quantitive investigation of Vortical Structures in the Near-Exit Region of an Axisymmetric Turbulent Jet,’ J. Turbulence, **9**, 19, pp. 1-20.

[9] Ganapathisubramani, B., Longmire, E. K., and Marusic, I., 2002, ‘Investigation of Three Dimensionality in the Near Field of a Round Jet Using Stereo PIV,’ J. Turbulence, **3**, 16, pp. 1-12.

[10] Olsson, M., Fuchs, L., 1996, ‘Large Eddy Simulation of the Proximal Region of a Spatially Developing Circular Jet,’ Phy. Fluids, **8**, 8, pp. 2125-2137.

[11] Bing, W., Huiqiang, Z., and Xilin, W., 2010, ‘Large-eddy Simulation of Near-field Dynamics in a Particle-laden Round Turbulent Jet,’ J. Aeronautics, **23**, pp. 162-169.

[12] Bogey, C., and Bailly, C., 2006, ‘Large Eddy Simulations of Transitional Round Jets: Influence of the Reynolds Number on Flow Development and Energy Dissipation,’ Phy. Fluids, **18**, pp. 1-14.

[13] Jorgensen, F. E., 2002, ‘How to measure turbulence with hot-wire anemometers – a practical guide,’ Dantec Dynamics, pp. 1-54.

[14] Taylor, Z.J.; Gurka, R.; Kopp, G.A.; Liberzon, A.; , "Long-Duration Time-Resolved PIV to Study Unsteady Aerodynamics," Instrumentation and Measurement, IEEE Transactions on , vol.59, no.12, pp.3262-3269, Dec. 2010 doi: 10.1109/TIM.2010.2047149 URL: http://ieeexplore.ieee.org/stamp/stamp.jsp?tp=&arnumber=5454643&isnumber=5609237

[15] Xu, G., and Antonia, R., 2002, ‘Effect of different initial conditions on a turbulent round free jet,’ Experiments in Fluids, **33**, 5, pp. 677-683.

◈◈◈